Available online at www.sciencedirect.com
ScienceDirect
Journal of Applied Geophysics 64 (2008) 37–46
JOURNAL OF APPLIED GEOPHYSICS
www.elsevier.com/locate/jappgeo

Rapid evaluation of multifrequency EMI data to characterize buried structures at a historical Jesuit Mission in Argentina

M.V. Bongiovanni, N. Bonomo, M. de la Vega, L. Martino, A. Osella *

Dpto. Física - Facultad de Ciencias Exactas y Naturales - Universidad de Buenos Aires - CONICET Ciudad Universitaria, Pab. I, 1428 Buenos Aires, Argentina

Received 6 February 2007; accepted 14 November 2007

Abstract

We present results from a geophysical prospection at a historical Jesuit Mission, located in San Ignacio (Misiones-Argentina), declared World Monument some years ago. We studied different sectors looking for buried structures; the total area under study covered 36 ha. In this work we will show the results obtained in a sector that at the time of the prospection was at imminent risk of being damaged by a wrong management of the historical resource. To optimize the data acquisition and the preliminary in-situ analysis of the results, we performed an electromagnetic survey using a multifrequency electromagnetic induction device (GEM-2) to have a first insight of the near surface electrical distribution. From 2D and 3D visualization of data, different targets were identified as possible historical structures. Around these anomalous zones, we performed different dipole–dipole profiles, forming high resolution grids for later 3D inversions. Further inversions of the electric and electromagnetic data completed the characterization of the anomalies. One of the main results of this work is that the 3D electric image obtained from 1D inversion of electromagnetic data coincides with the 3D images obtained from resistivity inversion, but at a much less time consuming cost.

Keywords: Near surface prospecting; 3D-electrical imaging; Electromagnetic inversion; Archaeological prospecting

1. Introduction

Geophysical surveys can provide important information to the archaeological community pertaining to the exploration and characterization of archaeological underground sites, in particular, the detection and localization of anthropological structures. Electromagnetic and electrical methods have been applied as pre-excavation techniques for many years since they posses high lateral resolution for shallow depths of study.

Geophysical methods are often applied to obtain 2D electrical images of the subsoil. More recently, 3D images are also being obtained, in which case a dense measurement grid is required. If the area to be surveyed is large and the target is located near surface, the 3D acquisition process could become excessively time expensive with traditional deployments. In that case, it is necessary to modify the design of the data acquisition. Techniques including 2D and 3D data visualization are valuable tools for near real-time (i.e., same day) analysis, since it can provide a preliminary diagnosis and guide further data acquisition; we have to take into account that usually the amount of data makes the possibility of 3D inversion impractical during the field work.

A usual strategy to map an extended area is to first apply a method that provides a quick qualitative location of anomalies (such as GPR or EMI methods). Once the anomalies have been identified from visualization of the data, a quantitative analysis can be done in selected areas. In these zones, methods that allow the inversion of data are applied to obtain 2D or 3D images of the subsoil, with the consequent localization of the targets. Geoelectrical methods are especially suitable for detailed quantitative analysis since there are many proven 2D and 3D inversion codes available that can produce high-resolution electrical images of the subsoil. This methodology has previously enabled us to characterize different archeological and environmental targets (Osella et al., 2005; Martino et al., 2006).

* Corresponding author. Fax: +54 11 4576 3357.
E-mail address: osella@df.uba.ar (A. Osella).

0926-9851/$ - see front matter © 2007 Elsevier B.V. All rights reserved.
doi:10.1016/j.jappgeo.2007.11.006

When the area to survey is large and targets are distributed in different sectors, acquiring gridded 3D dipole–dipole data over each possible anomaly can easily become too time consuming. This problem arose when we planned a geophysical prospection at a historical Jesuit Mission, located in San Ignacio (Misiones-Argentina), which was declared a World Heritage site by UNESCO in 1984. The total area under study covers 36 ha, different sectors of which (especially those with below-ground remains) are at risk of being damaged by inappropriate administration of the historical resource.

To optimize the data acquisition and the preliminary analysis of the results, we first conducted an electromagnetic survey using a multifrequency electromagnetic induction (EMI) device. The EMI data provided primary insight into the near surface electrical conductivity distribution. This kind of equipment is often used as a detector of conductive buried bodies (e.g., Witten et al., 2003). In recent years, several methods to calculate the EMI responses of metallic bodies have been presented, and applied to analyze and characterize the response of unexploded ordnance — UXO (e.g. Shubitidze et al., 2002; Sun et al., 2004). In these two studies it is supposed that the objects are located in free-space. This assumption can be done because metals usually are orders of magnitude more conductive than common background media. In these cases of very high conductive bodies, accurate numerical solutions are difficult to obtain and require extensive computation costs; moreover if we take into account that the calculation of the inductive response of the ground to a magnetic dipole source is a particularly complex subject. Despite this, many studies have been done to analyze and characterize the electromagnetic responses of conductive bodies (e.g., Won et al., 2001; Shubitidze et al., 2004).

On the other hand, when applied to archaeological targets, the background cannot be disregarded, since there are not usually large contrasts in the electrical resistivity. In a previous paper (Martinelli et al., 2006), we reported a forward modeling technique based on a Rayleigh–Fourier approach for 2D multi-layer structures and we showed that EMI method can be successfully applied to detect resistive structures. In fact, we applied this method to interpret data from archaeological targets. Also, 2D and 3D inversion methods have been developed to re-construct the conductivity profiles from EMI data, in the absence of highly conductive targets (e.g. Pérez-Flores et al., 2001; Haber et al., 2004; Sasaki and Meju, 2006), but they are usually applied to scales larger than the one required for near surface studies. For archaeological targets, we have to map large areas with high resolution both laterally and in depth. These conditions imply such amount of data that make 3D or even 2D inversion too time consuming, and then 1D methods, which are extremely fast (e.g., Huang and Won, 2000; Zhang and Liu, 2001; Farquharson et al. 2003) could be more adequate to have a rapid evaluation of data.

In this context, we analyze in the present paper whether more information could be obtained from the EMI data by performing a 1D inversion of the data. Our objective is to study the possibility of avoiding 3D dipole–dipole surveys, thus reducing the duration of the field work, but without losing resolution.

To address this objective, we selected one of the areas in San Ignacio Mini Mission where we performed EMI surveys. From the visualization of the data, we identified several possible anomalous zones. We selected one of these anomalous zones and performed a dipole–dipole 3D-survey. Then, the EMI data were inverted using a 1D inversion code and a 3D image was constructed by stitching together the 1D results. On the other hand, the dipole–dipole data were inverted using a 3D inversion code. Finally, we compared the electrical images obtained from both kinds of data.

2. The site

The Jesuit Mission in its present location dates from 1695. It was constructed in the Misiones jungle, and was completely abandoned by 1821. Misiones, the province where it was established, is known as 'the red land province' due to the clay contents of its soil. Walls were made of basalt rocks found in the nearby Parana river, with tile roofs over wood supports, and mud floors. The region has a subtropical climate without a dry season. The jungle covered the Mission as soon as it was abandoned. The town of San Ignacio developed around the ruins of the Jesuit Mission overlapping in part with it. Parts of the ruins were recovered from the jungle during the 1940s; but at that time many original constructions of San Ignacio were made using the materials of the ruins. Different activities related to the town have been held at various times at the site.

The map of the Jesuit Mission, with the structures that are now exposed, is shown in Fig. 1. The main buildings correspond to the church and the cloisters. The regular grids of structures were used as accommodation. These houses are all of the same size, approximately 4 m-wide, and feature columns, separated by 2 m from the external walls, which supported the roofs of the galleys that surrounded the houses (Fig. 2). The shadowed area shown in Fig. 1 named Sector 1, corresponds to one of the area with geophysical data. This area is now the entrance to the information office and there are plans to extend the administration buildings with the consequent risk of damaging possible buried structures. Therefore we studied this zone in order to characterize any remains still buried.

3. Methodology

Taking into account the characteristics of the previously described site, we expected to find resistive archaeological targets embedded in a conductive soil matrix. We first covered the area with an electromagnetic induction (EMI) survey. Electromagnetic techniques allow mapping of the electrical resistivity of the ground. One of their main advantages is that the process does not require direct contact with the ground and therefore is much faster than traditional geoelectrical methods.

We used a multifrequency electromagnetic induction profiler. This system consists of two small coils, a transmitter (*Tx*) and a receiver (*Rx*), separated by a constant distance (1.66 m), which are moved laterally along a profile. The secondary field detected at the receiver is decomposed into in-phase (H_I) and quadrature (H_Q) components, both of which are expressed in PPM (parts per million) of the primary field. The in-phase component depends mainly on the magnetic susceptibility (χ) of the media (e.g.

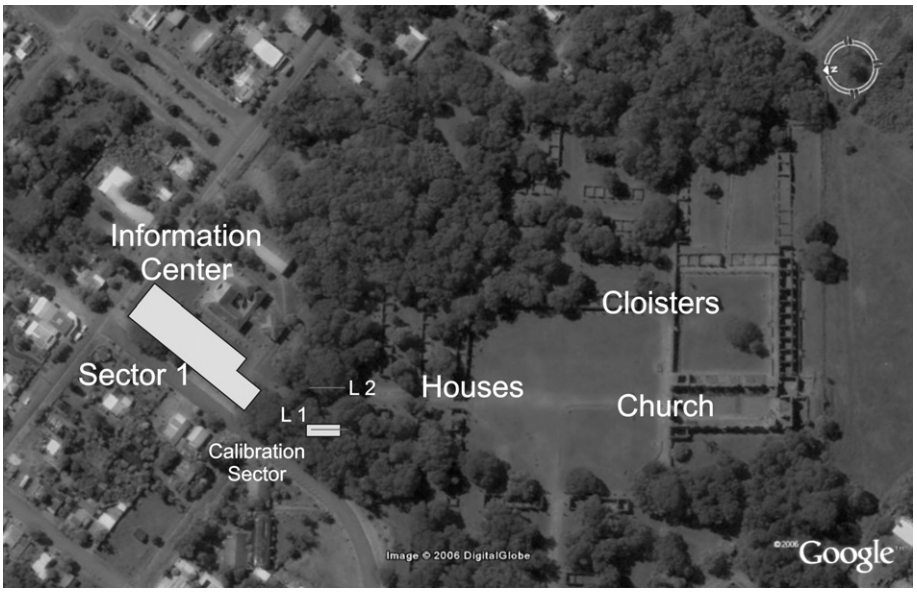

Fig. 1. Map of the San Ignacio Mini Jesuit Mission. The shadowed zones correspond to the calibration sector and the studied sector, named Sector 1. Lines L1 and L2 correspond to the dipole–dipole profiles, done for calibration.

Reynolds, 1997; Martinelli et al., 2006) and therefore this component is especially sensitive to metallic objects. The quadrature component is related to the distribution of electrical conductivity and may be converted to apparent conductivity, as a function of frequency, Freq, through the expression: $\sigma_a = 0.360 * H_Q(\mathrm{PPM})/\mathrm{Freq}$ (S/m) (Won et al., 1996). In this way, a visualization of the data provides insight into the electrical characteristics of the area such that possible anomalies can be identified.

The depth of penetration is a function of frequency and soil conductivity. Due to the range of frequencies involved, penetration is governed by the skin-depth $\delta = (2/\omega\sigma\mu)^{1/2}$, where ω is the angular frequency (2πFreq), σ is the conductivity of the medium, and μ is the magnetic permeability. Since the skin-depth formula is strictly valid for plane waves, δ gives an approximate depth of penetration that over-estimates the actual value.

For the present work we used the Geophex GEM-2 equipment (Won et al., 1996), which has a frequency range from 330 to 47,970 Hz, allowing a maximum of 15 survey frequencies, though usually 6 frequencies were used to guarantee good signal-to-noise ratio. As our target depths were expected to be 2–

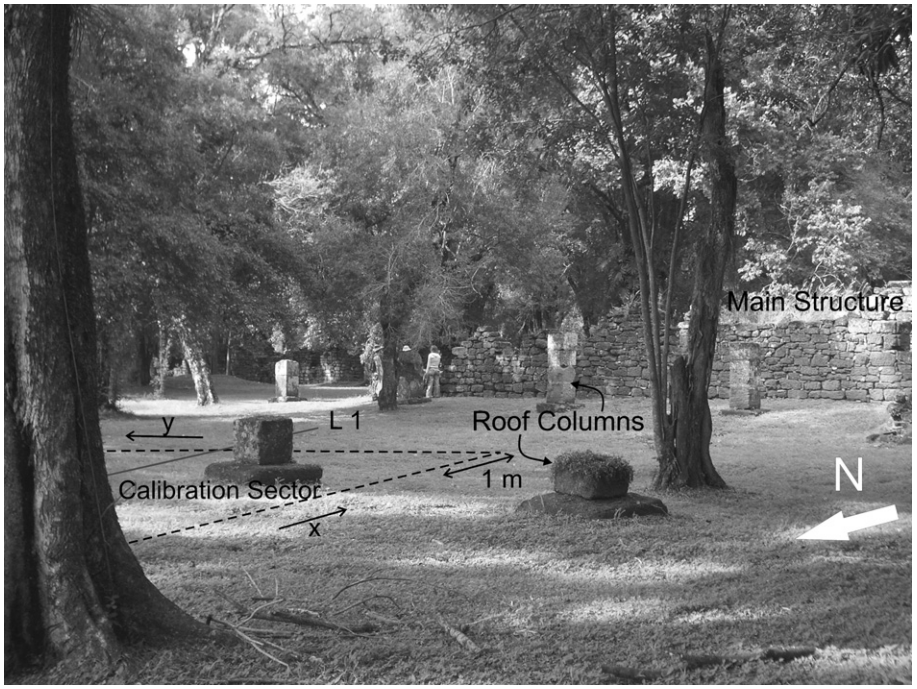

Fig. 2. Photo corresponding to the calibration sector (marked in a dashed black line). The dipole–dipole line L1 is also shown (solid trace).

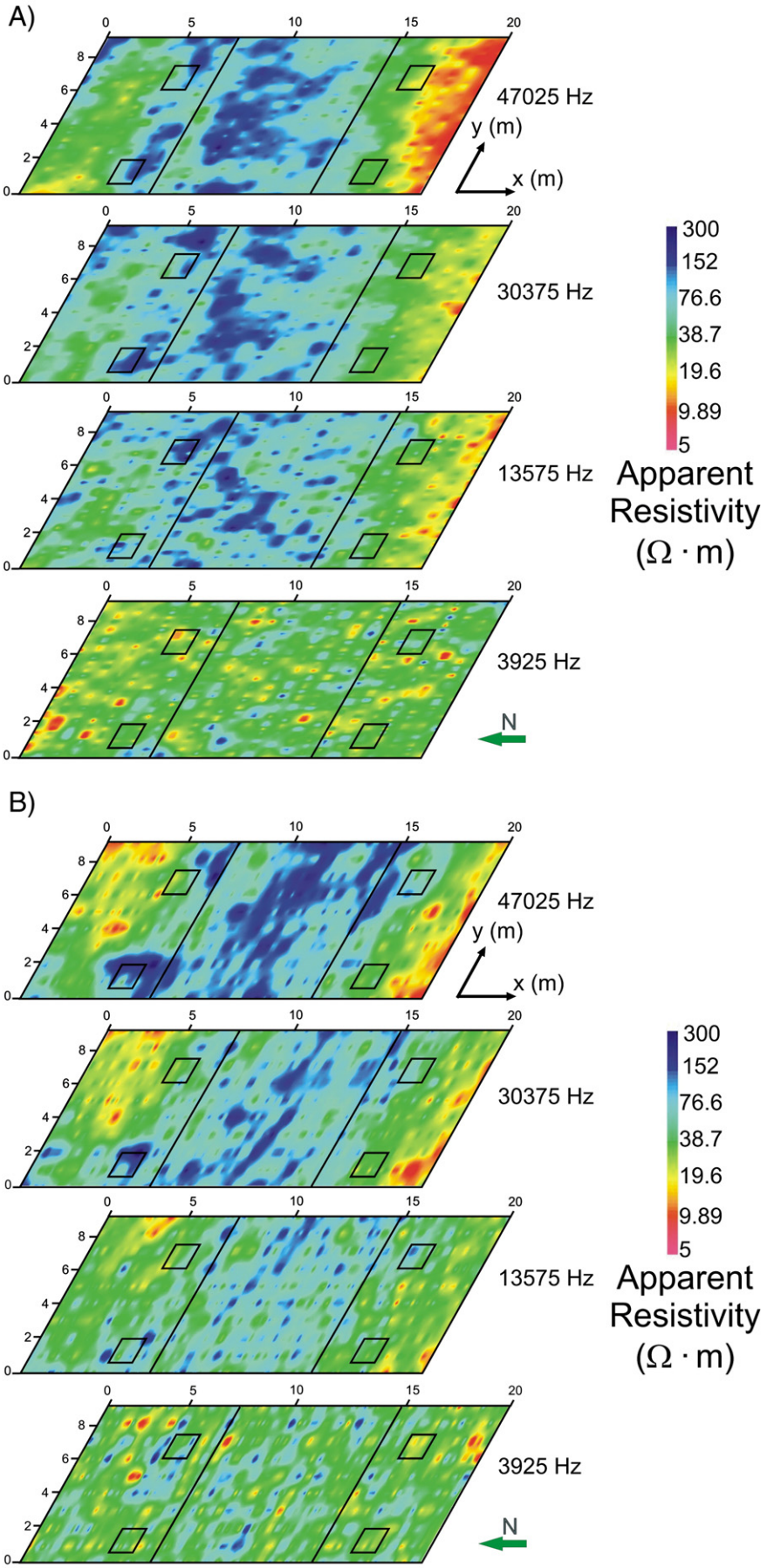

Fig. 3. Visualization of EMI data, obtained at the calibration sector, for four different frequencies: (A) surveys along *x*-direction, (B) surveys along *y*-direction. Solid lines indicate the limits of the expected house and the locations of the columns.

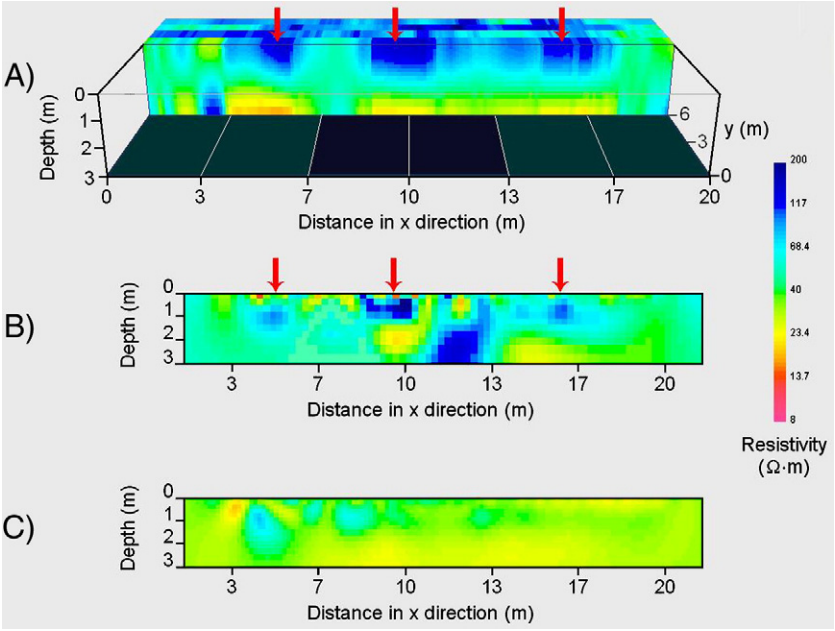

Fig. 4. (A) Cut at $y=6$ m of the 3D reconstruction from the 1D inversion of the EMI data. (B) 2D electrical image obtained from the inversion of dipole–dipole lines deployed crossing the structure close to the base of the columns. Arrows indicate the location of the columns and the basement. (C) 2D electrical image obtained from L2.

3 m, we selected the six frequencies: 2575, 3925, 8775, 13,575, 30,375 and 47,025 Hz. We performed in-line surveys (*Tx–Rx* azimuth coincident with the direction of survey lines), with the dipole axes perpendicular to the ground. The line spacing in each EMI-surveyed sector is 1 m. Data were collected in two orthogonal directions in a quasi "continuous mode", which in fact implies one measurement each approximately 0.10 m. The visualization of data was performed through plan-view maps of apparent resistivity for each frequency. The data collected along each profile were inverted using a 1D inversion code, EM1D v1.0, (Farquharson et al., 2003). We first applied smoothness constrains to remove outliers that distort the inversion procedure. Then, the resulting inverted 1D models were stitched-together to build up a pseudo-3D electrical image.

As stated previously, dipole–dipole profiles were also acquired in specific locations, to be used as a test for the reliability of the images obtained from 1D inversion of the EMI data. The electrical surveys were performed using the multielectrode resistivimeter Saris 500. We deployed dipole–dipole arrays with electrode separations of 0.5 m and 1 m. To obtain electrical tomograms, data were inverted using the DCIP2D and DCIP3D inversion codes developed at the University of British Columbia (UBC) by Oldenburg et al. (1993) and Oldenburg and Li (1994).

For each inversion of dipole–dipole and EMI data, we also estimated the depth of investigation of the profile using the method of Oldenburg and Yaoguo (1999). By inverting the data with different model inputs (reference or initial conductivity model) and comparing the resulting images, we estimate the depth above which the resulting models are independent of the initial parameters. In this way, we determine which part of the model obtained from the inversion of the field data reliably represents the subsoil. We followed this procedure for each profile. In all cases the depth of investigation was larger than 3 m. This depth fulfilled our requirements since no archaeological remains were found deeper than 2 m.

4. Calibration tests

To identify typical patterns of anomalies from the targets of interest, we performed test surveys on a sector where buried structures are known to exist. We selected a sector, shown in Fig. 1 as calibration sector, where the base of columns remained exposed. The walls of the house no longer exist, but the basement appeared in an excavation-test at approximately 0.5 m deep. Part of this sector is marked in Fig. 2.

The EMI profiles were acquired along both the *x*- and *y*-directions (Fig. 2). A total of 11 *x*-profiles and 21 *y*-profiles were carried out, covering the entire calibration sector. We also acquired two dipole–dipole profiles, one at $y=6$ m (L1), within the house zone, and the other outside the zone of the houses (L2, see Fig. 1).

In Fig. 3 the visualization of EMI data in the form of apparent resistivity, $\rho_a = 1/\sigma_a$ at four frequencies, for *x*- and *y*-profiles (Fig. 3A and 3B, respectively) is shown. In this figure, full black lines indicate the expected limits of the house (assuming that all the houses kept the same construction design) and the location of the columns. The plan-view maps for each frequency show interesting features. One of the main results is the coincidence between the responses for the *x*- and *y*-configurations. It suggests that the anomalies might be produced by a structure extended relative to the grid dimension, since a localized elongated body would produce different responses depending on the direction of the survey. We can also see that a resistive response appears in the zone where the house basement is embedded; this pattern appears for both configurations, up to frequency 8775 Hz (not shown in the figure, since it is similar to the response at

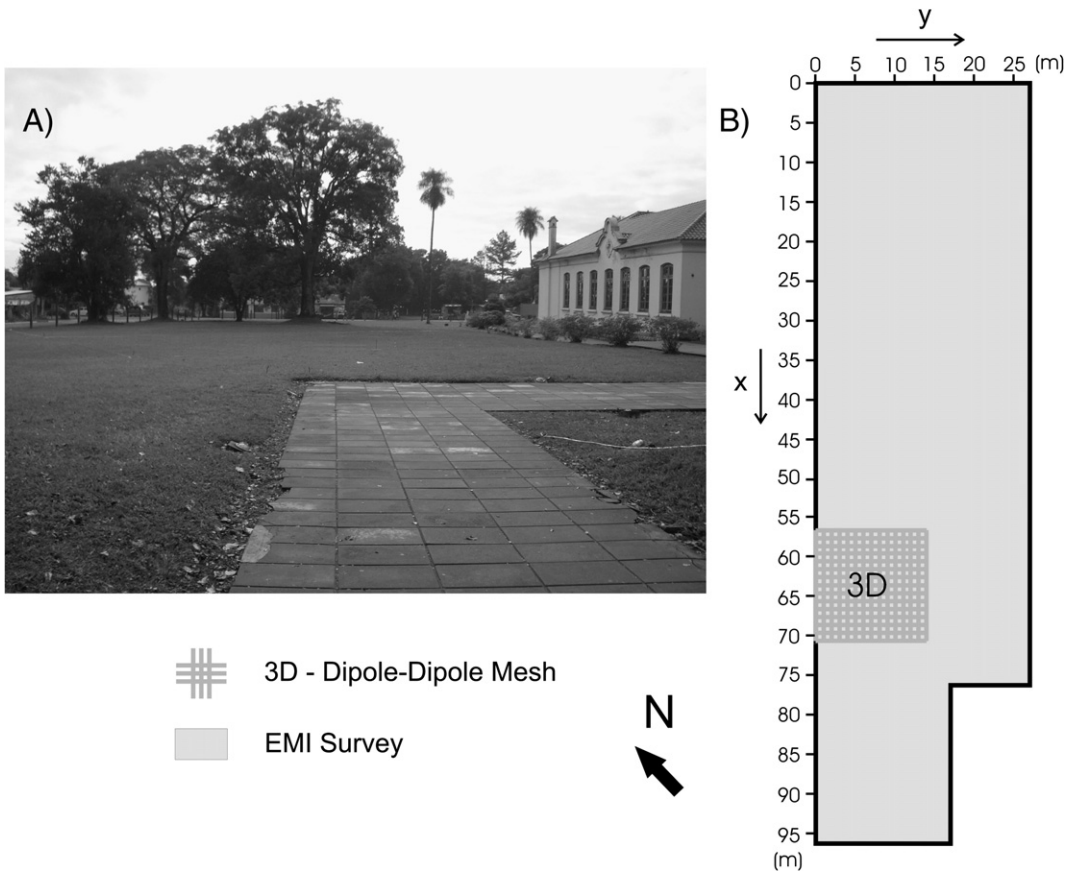

Fig. 5. (A) Photo corresponding to the studied sector. (B) Schema of the area covered with the EMI surveys. The darker zone corresponded to the 3D dipole–dipole array.

13,575 Hz). The lowest two frequencies presented similar responses; we only show the map corresponding to 3925 Hz.

We then inverted the EMI and the dipole–dipole data. As the lowest EMI frequency data contains too much error due to noise (the amplitude of the response decrease with frequency), we did not use it for inversion. Fig. 4A shows a cut at $y=6$ m of the 3D reconstruction from the 1D inversions of the EMI data. Fig. 4B shows the 2D electrical image obtained from the inversion of a dipole–dipole line deployed crossing the structure, also at $y=6$ m. Arrows indicate the location of the columns and the basement. The agreement between the EMI and dipole–dipole inversions is remarkable. As a comparison, we show in Fig. 4C the electrical imaging corresponding to L2, outside the zone of the houses. The behavior here is different from that observed at L1. We conclude that, when prospecting for archaeological targets in areas where there is no evidence at the surface, we must look for resistive anomalies. The same patterns are obtained using either electric or electromagnetic methods.

5. Results

We further studied the sector shown in Fig. 1, close to the information center of the site. Fig. 5A shows a photo of the sector. It can be seen that the place has been modified (including buried pipes related to electricity and water disposal). In Fig. 5B we display the acquisition scheme of the sector which is covered with EMI measurements. Also shown is the grid where the 3D dipole–dipole survey was acquired.

Following the earlier procedures at the calibration sector, we first performed EMI surveys along lines both in the x- and y-directions. In Fig. 6 we present the results for four frequencies. As in the previous case, the plan-view maps for the different frequencies are similar for soundings along the x- and y-directions (Fig. 6A and B, respectively). The remarkable features are the resistive anomalies which follow an approximately regular array, with a separation similar to that observed between the exposed houses. Moreover, the values for the apparent resistivity are of the same order as the ones obtained in the calibration sector (Fig. 3), for both the resistive anomalies and the surrounding soil.

We then inverted the data using the EM1D code. As an example, we show in Fig. 7 the electrical image obtained from the inversion of line $x=10$ m (Fig. 7B) together with the fitting of the model response to data. After inverting all the profiles, we built up the 3D model. For this model we did not include the sector between $y=77$–97 m, since the data were distorted by the presence of an iron pipe. This kind of object cannot be correctly modeled during a 1D inversion. Fig. 8A shows the results; for a better visualization of the anomalous structures we removed the first layer, approximately 10 cm; Fig. 8B shows a skew cut, where the depths of the anomalous structures can be observed.

Based on the previous results, we selected the sector to perform a 3D imaging from dipole–dipole data. We used a grid

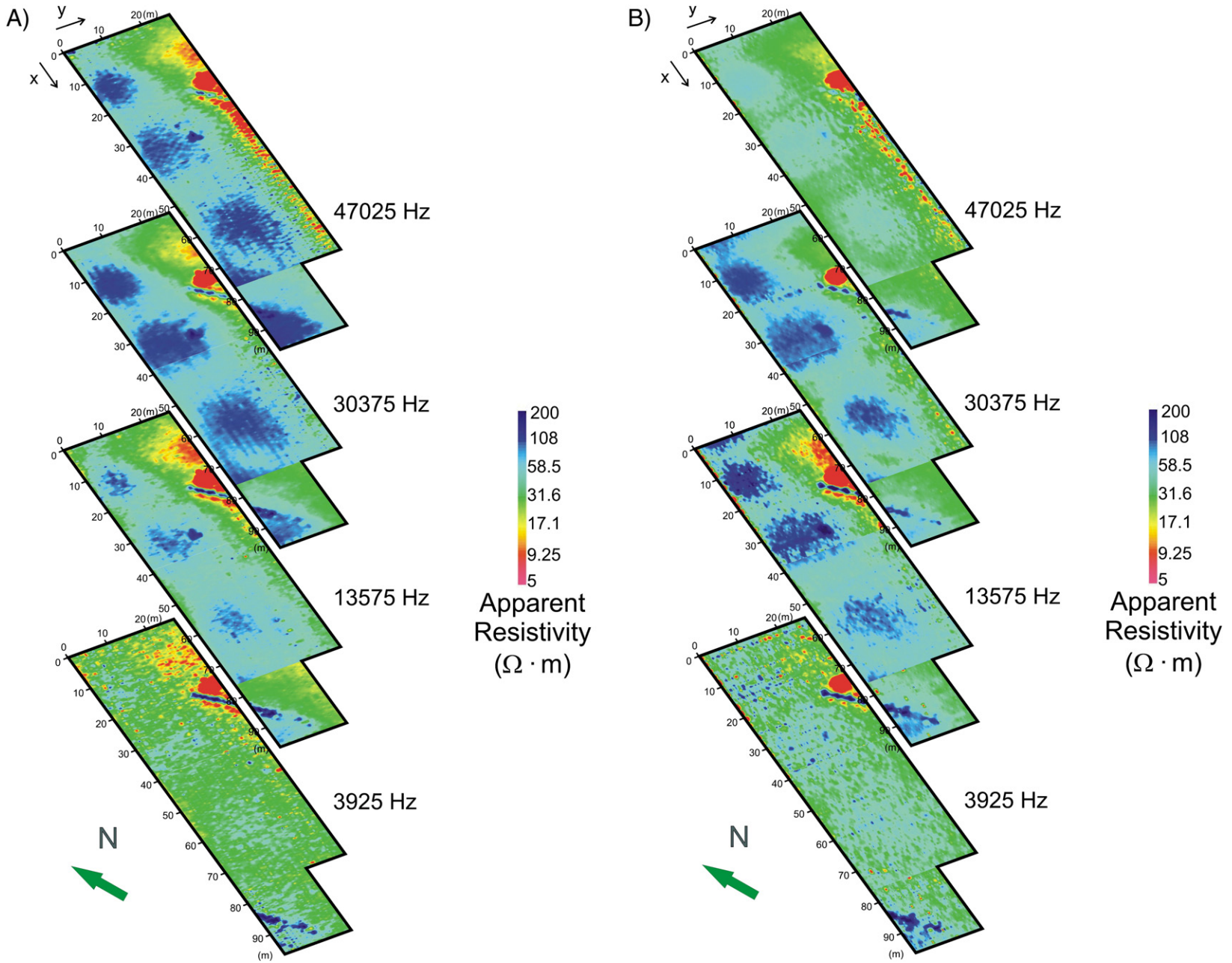

Fig. 6. Visualization of EMI data, obtained at the studied sector, for four different frequencies: (A) surveys along *x*-direction, (B) surveys along *y*-direction.

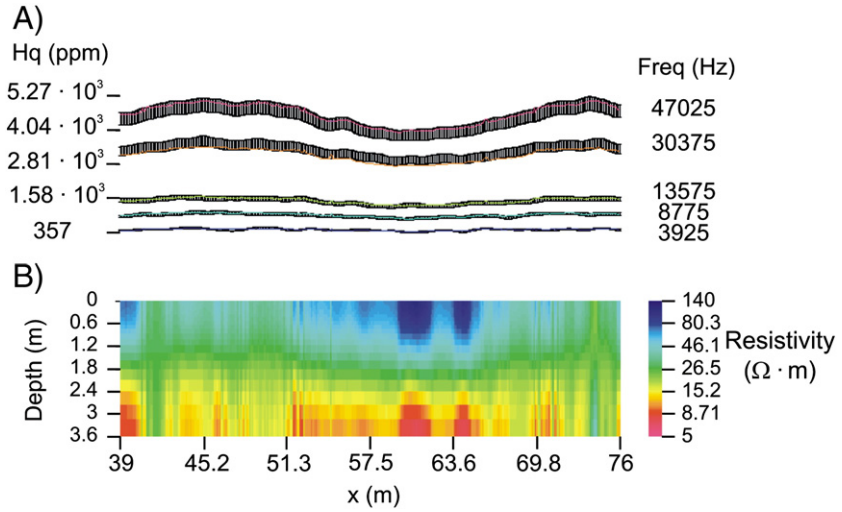

Fig. 7. Inversion of EMI data along $x=10$ m profile. (A) Fitting of data and (B) resulting electrical imaging.

with cells of 1×1 m, and deployed dipole–dipole lines, with a maximum $n=6$, in both directions (Fig. 6B). The inversion was done using the DCIP3D code; the result is shown in Fig. 9. A plan-view map at $z=0.90$ m (Fig. 9A) shows the anomalous zone, again in coincidence with the image obtained from the EMI data. To characterize the depth of the structure, a cut at $y=63$ m is presented (Fig. 9B).

We next compare the results obtained at the calibration sector with the electrical images obtained here. We see that possible structures or bodies associated with the archaeological materials that form the basement of the houses and columns should have electrical resistivities larger than 90 Ω m. The 3D image obtained from the dipole–dipole data agreed with the model built up with the 1D inversion of the EMI data, thus providing confirmation of the predicted anomalous bodies. We removed from the electrical image given in Fig. 8 resistivities lower than 80 Ω m, in order to isolate the possible anomalous materials. When doing this (see Fig. 10), the effect is remarkable. We can clearly characterize three blocks of resistive material, separated by regular distances. While these anomalous bodies could be detected from the visualization of the data, quantitative inversion better constrains the depths, which are important for preservation tasks. We can go one step further and try to identify these structures. The original purpose of the study in this sector was to look for evidence of remains of houses. It is known that at the time that the Mission was operational, many more houses were present than the ones exposed today (as shown in Fig. 1). It is also known that

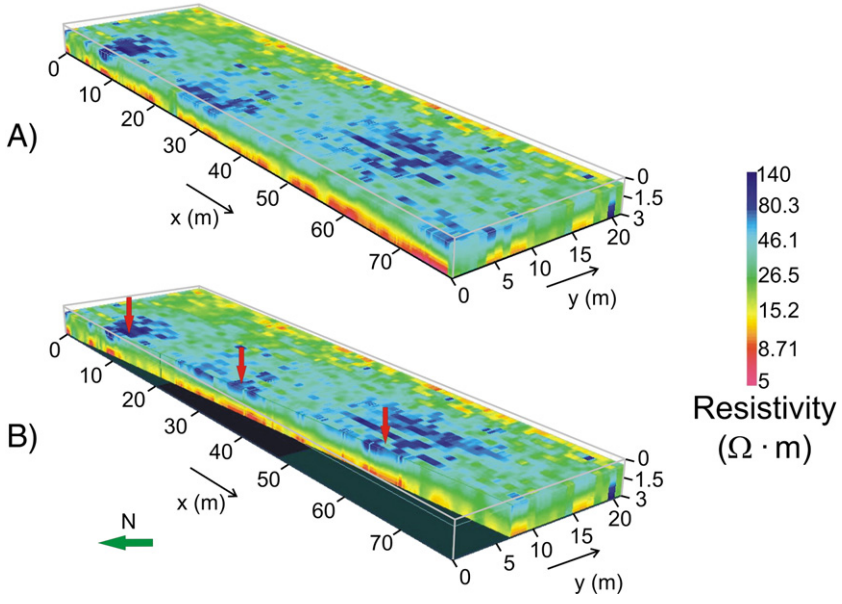

Fig. 8. (A) 3D reconstruction from the 1D inversion of the EMI data at the studied sector and (B) skew cut, showing the depth of the structure.

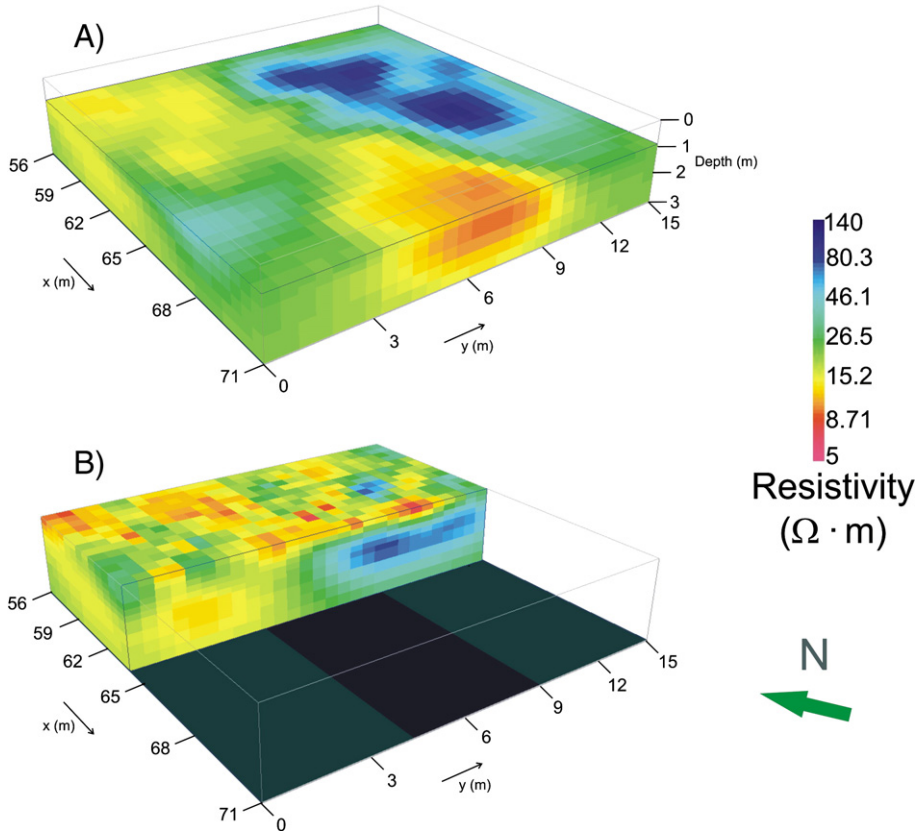

Fig. 9. (A) 3D electrical imaging, obtained from the inversion of the dipole–dipole data, corresponding to the area showed in Fig. 5B and (B) a cut showing location in depth of the anomalous body.

these houses were constructed following a certain order with, essentially, a repetitive plan. Therefore, we assume a regular continuation of the houses over this sector that follows the existing design; the projected structures are fully superimposed on the anomaly map in Fig. 10. The result clearly explains our observations.

The geophysical results were used to draw up a plan for text-excavations, which was subsequently carried out. The predicted basements were found, and nowadays, works are being carried out to preserve the Jesuit Mission from future damages.

6. Conclusions

We faced the problem of characterizing a human-impacted site, prospecting for shallow resistive targets, embedded in a conductive host soil. To reduce the field work involved without sacrificing resolution, we studied the possibility of using EMI data to obtain 3D electric images. We studied in detail a sub-sector of the site, in which buried structures were expected. A thorough survey of this zone was performed using EMI and resistivity methods. A 1D inversion of EMI data allowed us

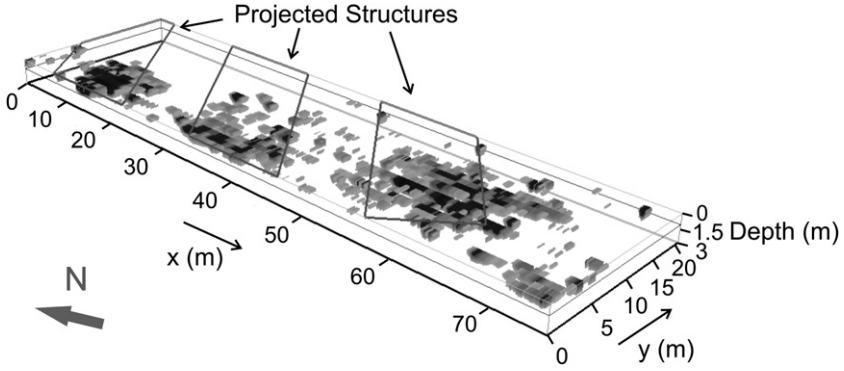

Fig. 10. Localization of anomalous resistive bodies. Solid lines correspond to the location of predicted structures obtained as a continuation of the exposed houses (from Fig. 1).

obtain a 3D reconstructed electric image of the zone. This image was compared with the electric image obtained from 3D inversion of dipole–dipole data. The electrical images obtained from both datasets are highly correlated. Therefore, an accurate prediction of the subsurface can be obtained from the less time consuming electromagnetic method.

It is well-known that 2D or 3D models can better reproduce an actual structure than 1D model, which cannot determine univocally thickness and resistivity of each layer. But 1D inversion codes have the very important advantage of being extremely fast, and then are especially suitable when dealing with large amount of data. Notice that just in the calibration sector we had 10 lines, each one with a length of 20 m, and data each 0.10 m. This implied that in an area of 10 m × 20 m, for example, we had 2000 "stations" to be used for the inversion. This number is far beyond the capability of a 2D or 3D inversion method. Nevertheless we found that the inherent ambiguity in 1D models could be overcome by the dense grid of measurements, and thus the 1D inversion of EMI data and further stitching together 1D models to produce a 3D image provided a result compatible with 3D inversion of dipole–dipole data. Though better resolution is acquired in this last case, we reduced the time spent in the field. We must take into account that the 3D dipole–dipole grid of 15 m × 15 m took one day of work. The EMI survey covered, in the same time, a sector of 95 m × 25 m approximately plus the calibration sector of 10 m × 20 m. This is an important issue, since we had to cover many sectors of the site and we could not afford the time required for a full geoelectrical prospection.

Acknowledgments

This work was supported by the ANPCyT (Agencia Nacional de Promoción Científica y Tecnológica) and World Monuments Funds Foundation.

References

Farquharson, C.G., Oldenburgh, D.W., Routh, P.S., 2003. Simultaneous 1D inversion of loop–loop electromagnetic data for magnetic susceptibility and electrical conductivity. Geophysics 68 (6), 1857–1869.

Haber, E., Ascher, U.M., Oldenburg, D.W., 2004. Inversion of 3D electromagnetic data in frequency and time domain using an inexact all-at-once approach. Geophysics 69 (5), 1216–1228.

Huang, H., Won, I., 2000. Conductivity and susceptibility mapping using broadband electromagnetic sensors. Journal of Environmental and Engineering Geophysics 5 (4), 31–41.

Martinelli, P., Osella, A., Lascano, E., 2006. Modeling broadband electromagnetic induction responses of 2-D multilayered structures. IEEE Geoscience and Remote Sensing 44 (9), 2454–2460.

Martino, L., B., N., Lascano, E., Osella, A., Ratto, N., 2006. Electrical and GPR joint prospecting at the Palo Blanco archaelogical site, NW Argentina. Geophysics 71 (6), 193–199.

Oldenburg, D.W., McGillivary, P.R., Ellis, R.G., 1993. Generalized subspace method for large scale inverse problems. Geophysical Journal International 114, 12–20.

Pérez-Flores, M.A., Méndez-Delgado, S., Gómez-Treviño, E., 2001. Imaging low-frequency and dc electromagnetic fields using a simple linear approximation. Geophysics 66 (4), 1067–1081.

Oldenburg, D.W., Li, Y., 1994. Inversion of induced polarization data. Geophysics 59, 1327–1341.

Oldenburg, D.W., Yaoguo, L., 1999. Estimating depth of investigation in dc resistivity and IP surveys. Geophysics 64 (2), 403–416.

Osella, A., dela Vega, M., Lascano, E., 2005. 3D electrical imaging of an archaeological site using electric and electromagnetic methods. Geophysics 70 (4), 101–107.

Reynolds, J.M., 1997. An Introduction to Applied and Environmental Geophysics. John Wiley & Sons Eds., 796 pp.

Sasaki, Y., Meju, M.A., 2006. A multidimensional horizontal-loop controlled-source electromagnetic inversion method and its use to characterize heterogeneity in aquiferous fractured crystalline rocks. Geophysical Journal International 166, 59–66.

Shubitidze, F., O'Neill, K., Haider, S.A., Sun, K., Paulsen, K.D., 2002. Application of the method of auxiliary sources to the wide-band electromagnetic induction problem. IEEE Geoscience and Remote Sensing 40 (4), 928–942.

Shubitidze, F., O'Neill, K., Sun, K., Paulsen, K., 2004. Investigation of broadband electromagnetic induction scattering by highly conductive, permeable, arbitrarily shaped 3D objects. IEEE Geoscience and Remote Sensing 42 (3), 540–556.

Sun, K., O'Neill, K., Shubitidze, F., Shamatava, I., Paulsen, K.D., 2004. Theoretical analysis and range of validity of TSA formulation for application to UXO discrimination. IEEE Geoscience and Remote Sensing 42 (9), 1871–1881.

Witten, A., Calvert, G., Witten, B., Levy, T., 2003. Magnetic and electromagnetic induction studies at archaeological sites in Southwestern Jordan. Journal of Environmental and Engineering Geophysics 8 (3), 209–215.

Won, I.J., Kreiswetter, D.A., Fields, G.R.A., Sutton, L., 1996. GEM-2: a new multifrequency electromagnetic sensor. Journal of Environmental and Engineering Geophysics 1 (2), 129–137.

Won, I., Keiswtter, D., Bell, T., 2001. Electromagnetic induction spectroscopy for clearing landmines. IEEE Geoscience and Remote Sensing 39 (4), 703–709.

Zhang, Z., Liu, Q., 2001. Two nonlinear inverse methods for electromagnetic induction measurements. IEEE Geoscience and Remote Sensing 39 (6), 1331–1339.

Further-reading

DCIP2D V3.1, 2001. Forward modelling and inversion of DC resistivity and induced polarization data over 2D structures. UBC-Geophysical Inversion Facility.

DCIP3D V1.0, 2003. Forward modelling and inversion of DC resistivity and induced polarization data over 3D structures. UBC-Geophysical Inversion Facility.

EM1DFM V1.0, 2000. Inversion and modelling of applied geophysical electromagnetic data. UBC-Geophysical Inversion Facility.